

Observations of auroral medium frequency bursts

J. LaBelle, S. G. Shepherd, and M. L. Trimpi

Department of Physics and Astronomy, Dartmouth College, Hanover, New Hampshire

Abstract. Auroral medium frequency (MF) bursts are broadband impulsive radio emissions observed at ground level during the breakup phase of auroral substorms. Measurements made in northern Canada during 1995–1996 show the seasonal and local time dependencies of MF burst emissions, provide case-study evidence for a null in the MF burst spectrum near twice the ionospheric electron gyrofrequency, and establish a correlation between MF burst and impulsive auroral hiss. High time resolution measurements reveal that MF bursts occur in 100–300 μ s wave packets which sometimes appear periodic having a period close to the ionospheric proton gyroperiod. The timescales of the MF burst wave packets are comparable to those of whistler solitary waves recently observed with the FAST satellite.

1. Introduction

Radio waves at frequencies ranging from a fraction of a hertz to several megahertz are often associated with auroral displays. Although many auroral waves cannot escape the ionosphere and are only observed with rocket- or satellite-borne instruments, there are several types of waves which are detected at ground level. In the LF/MF/HF frequency range (30 kHz to 30 MHz), the most prominent auroral emissions observed at ground level are auroral hiss, medium frequency burst (MF burst), and auroral roar [e.g., *LaBelle et al.*, 1994]. MF burst is the least well described of these three phenomena. *Kellogg and Monson* [1979] observed occasional radio bursts at times when aurora was overhead, but these could not be reliably distinguished from lightning-generated atmospherics which could have been their source (P. J. Kellogg, personal communication, 1995). *Weatherwax et al.* [1994] reported the first definitive observations of MF burst, determined its approximate frequency range, provided statistical evidence for a null in the MF burst spectrum near twice the electron gyrofrequency, and suggested that MF burst and auroral hiss are correlated. Since the initial study, hundreds of MF burst emissions have been observed at many auroral zone locations. These new data provide better case study and statistical evidence of the characteristics of the emissions. In particular, high time resolution waveform measurements reveal that the durations of individual MF burst wave packets are the order of 100–300 μ s, much shorter than previously thought.

2. Instrumentation

Two types of radio receiver have been developed at Dartmouth College and deployed in Arctic and Antarctic observatories to record auroral MF burst emissions: a programmable frequency receiver and a downconverting receiver. Both receivers use the same preamplifier and antenna, a 10 m² magnetic loop oriented to optimize sensitivity to sky noise and to null out the strongest source of local interference. Antenna and preamplifier are located at least 100 m from the building containing the receivers.

The programmable receiver can be programmed to emphasize frequency or time resolution according to the desires of the experimenter. The normal program used for routine data collection sweeps 0.05–5.00 MHz each 2 s with 10-kHz resolution and operates 20 hours/d, skipping 4 hours around local noon for housekeeping purposes [*Weatherwax*, 1994]. The data are digitized in the computer, displayed on a monitor in real-time, and archived on streamer tapes or optical disks which are mailed to Dartmouth College for analysis. In stages between 1994 and 1996, Dartmouth installed these receivers in five Canadian CANOPUS observatories spanning invariant latitudes from 66° to 79° along a geomagnetic meridian and imbedded within the larger CANOPUS array of magnetometers, photometers, riometers, and all-sky imagers. Table 1 shows the locations and magnetic latitudes of these Canadian observing sites.

For a 3-week campaign at Churchill, Manitoba, in April 1996, two programmable receivers and a downconverting receiver were used. One programmable receiver, hereafter referred to as the normal programmable receiver (NPR), operated at the normal sample rate and bandwidth described above. The other, hereafter referred to as the fast programmable receiver (FPR), was programmed to measure signals at four selected 10-kHz-wide frequency bands at a 3-kHz sample rate; thus the

Copyright 1997 by the American Geophysical Union.

Paper number 97JA01905.
0148-0227/97/97JA-01905\$09.00

Table 1. Dartmouth College Radio Receiver Sites in Northern Canada

Site	Geographic Latitude	Geographic Longitude	Invariant Latitude	UT Corresponding to Midnight MLT
Gillam, Manitoba	56.38	265.36	66.8	0637
Churchill, Manitoba	58.76	265.92	69.2	0635
Arviat, Northwest Territories	61.11	265.95	71.4	0637
Baker Lake, Northwest Territories	64.32	263.97	74.2	0652
Taloyoak, Northwest Territories	69.54	266.45	79.2	0647

UT, universal time; MLT, magnetic local time.

receiver recorded a four-frequency spectrum each 1.2 ms. Three of the frequencies (2000, 2300, and 2600 kHz) were selected in the range of MF burst frequencies, and one frequency (430 kHz) was selected in the range of LF auroral hiss.

A tunable downconverting receiver was also used in the April 1996 campaign. The downconverting receiver translates a user selectable 10-kHz band, located at any frequency from 10 kHz to 5 MHz, to the frequency range 2–12 kHz which can be recorded on audio tapes. An analog filter at the tape recorder input compensates for the preemphasis filter built into the audio tape recorder, and an inverse filter applied upon playback produces an approximately equalized instrument response over the 2–12 kHz band. Data are recorded on 90-min audio tapes. The large quantity of data and the need to change tapes frequently make automatic operation difficult, although the first observations of auroral roar fine structure were recorded that way [LaBelle *et al.*, 1995]. In the April 1996 campaign, the downconverting receiver was tuned interactively based on the real-time programmable receiver data.

3. Data Presentation

Figure 1 shows auroral radio emissions recorded with the NPR at Churchill, Manitoba, and Arviat, NWT, during 0620–0715 UT (0020–0115 LT) on April 24, 1995. Arviat (71.4° invariant latitude) lies about 200 km north of Churchill (69.2° invariant latitude). At both stations, midnight magnetic local corresponds to about 0635 UT (0035 LT). The spectrograms cover 0–4 MHz on the vertical axis, with wave intensity encoded into the gray scale. (White pixels correspond to ≤ 4 nV/m $\sqrt{\text{Hz}}$ and black pixels correspond to ≥ 400 nV/m $\sqrt{\text{Hz}}$, respectively.) Dark horizontal lines represent fixed frequency transmissions such as those occurring in the AM broadcast band at 550–1600 kHz. The other panels display riometer and magnetometer data from the CANOPUS stations at Arviat, Churchill, and Gillam (66.8° invariant latitude).

Three types of LF/MF/HF auroral radio emissions are labeled in Figure 1a: Auroral roar occurs centered near 2.9 MHz between 0622 and 0650 UT, becoming intermittent thereafter; auroral hiss occurs below 1 MHz between 0651 UT and 0712 UT; and MF bursts are the broadband bursty waves starting at 0651 UT and covering the frequency range 1.5–3.8 MHz in this example.

The MF bursts recorded at Arviat show quite distinctly a null near 3 MHz, which is approximately twice the ionospheric electron gyrofrequency (f_{ce}). This example provides direct evidence of this spectral feature which was surmised by *Weatherwax et al.* [1994] based on statistical data. Most MF burst events occur either above or below $2f_{ce}$; individual events that extend both above and below $2f_{ce}$ are unusual but are characterized by a null in the spectrum near $2f_{ce}$ when they occur. The auroral roar continues to occur intermittently at approximately the same frequency as the gap in the MF burst spectrum, suggesting the possibility that auroral roar plays a role in the suppression of the MF burst signal. Statistics from many observatories at different latitudes prove that the auroral roar emission is associated with $2f_{ce}$; however, similar data are not available for the gap in the MF burst spectrum, which is less often observed. If the gap in the example of Figure 1a is associated with $2f_{ce}$, its frequency range (2.90–2.95 MHz) corresponds to 277–315 km above Arviat, assuming a dipole magnetic field.

Figure 1 also illustrates the correlation between MF burst and impulsive auroral hiss, which occurs at frequencies below ~ 1 MHz during substorm onsets (see reviews by *Hellwell* [1965] and *Sazhin et al.* [1993]). Both types of emissions consist of groups of impulsive emissions lasting 10–60 s. At least seven groups of MF burst impulses are recorded at Arviat between 0651 and 0712 UT, and these are correlated one-to-one with groups of auroral hiss impulses. The 2-s time resolution of these records is not sufficient to correlate individual impulses of MF burst with those of auroral hiss.

The MF burst signatures recorded at Arviat are strikingly different from those recorded at Churchill, 200 km south. No MF burst is observed at Churchill above the noise level of the instrument after 0652 UT, even though MF burst exceeding that noise level by up to 35 dB is observed at Arviat. Such dramatic differences between MF burst signals received 200 km apart are commonly observed. In Figure 1, the auroral roar signals observed at Churchill and Arviat appear nearly identical, but this observation is unusual; often, there are significant differences in auroral roar emissions observed at stations 200 km or more apart.

Like auroral hiss, MF burst characterizes the expansion phase of the auroral substorm. At 0645 UT, absorption of AM radio signals is observed at Churchill simultaneous with the onset of auroral hiss and MF

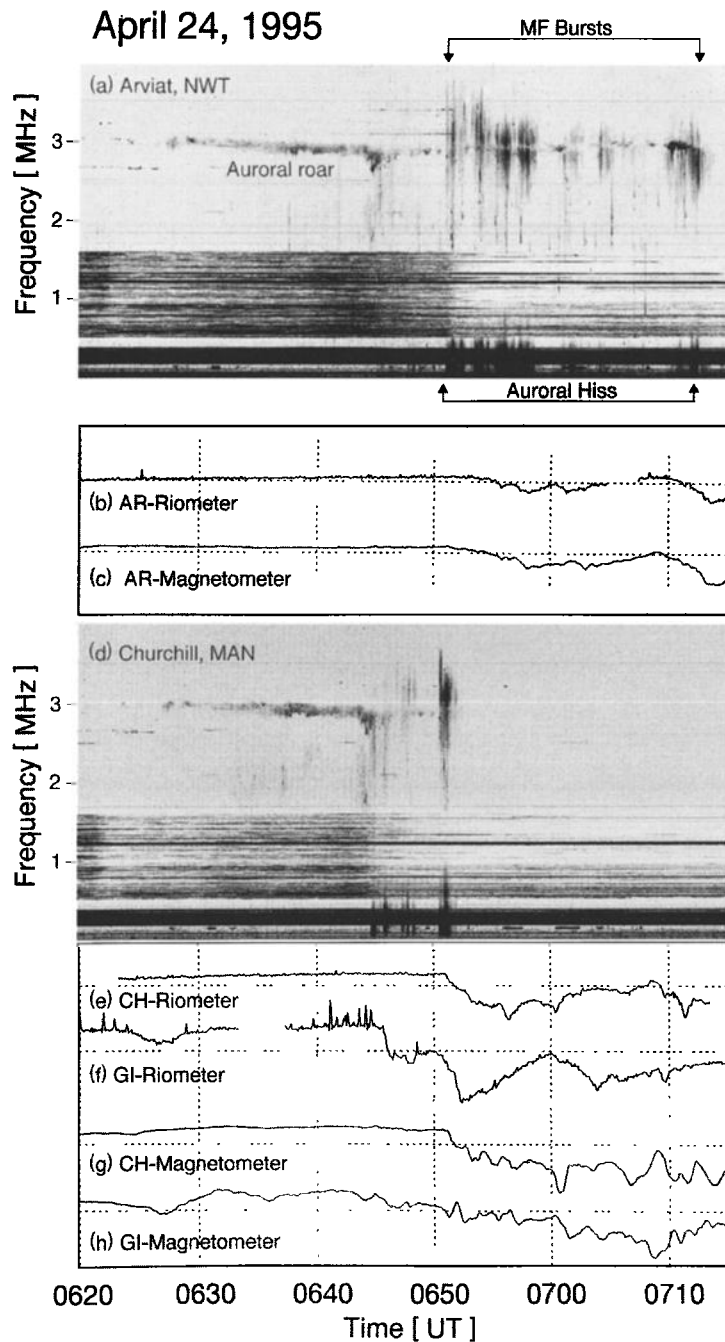


Figure 1. (a) A 0–4 MHz spectrogram recorded at Arviat, Northwest Territories, showing three types of auroral radio emissions: auroral roar, a narrowband emission near 3 MHz; MF burst, broadband emissions at 1.5–3.8 MHz starting at 0651 UT in this example, and auroral hiss, broadband emissions below 1 MHz; (b) 30-MHz riometer data and (c) H component magnetometer data recorded by CANOPUS instruments at Arviat; (d) A 0–4 MHz spectrogram recorded at Churchill, Manitoba, in the same format as Figure 1a. Lower panels show riometer and H component magnetometer data recorded by CANOPUS instrumentation at Churchill and Gillam, Manitoba.

burst. These same signatures, only weaker, are detected at Arviat. Initial prompt riometer absorption and deflections in magnetometer traces at two stations south of Churchill, Island Lake and Gillam, also occur at 0645 UT. At 0651 UT, the first large bay in the mag-

netic field H component is recorded locally at Churchill, accompanied by enhanced riometer absorption. At the same time, the most intense MF burst and auroral hiss up to 1 MHz occur at Churchill, deep absorption of AM broadcast band signals sets in at Arviat, and a

series of at least seven groups of MF bursts begins at Arviat. Local magnetometer and riometer activity at Arviat remains relatively low-level until about 0712 UT, at which time a magnetic bay and riometer absorption are observed coincident with MF burst and auroral hiss, preceded by a burst of auroral roar. After this time, no radio emissions are detected at either observatory. The disappearance or intermittency of auroral radio emissions observed at ground level after substorm breakup has been attributed to screening of the waves due to precipitation-induced ionization in the lower ionosphere below the wave source.

Figure 2 summarizes 6 months of MF burst observations, September 1994 through April 1995, at three CANOPUS sites: Gillam, Churchill, and Arviat. The vertical axis represents the number of nighttime hours during which at least one MF burst occurred, as a fraction of the total nighttime hours for which data were obtained. This ratio was measured every night, but the values plotted in Figure 2 have been averaged with a 7-day triangular sliding window. Gaps in the data from each station indicate periods when no data were available from that station. Despite these gaps, MF bursts are clearly less common at Gillam (66.8°) than they are at either Churchill (69.2°) or Arviat (71.4°), where occurrence rates are similar. As yet, insufficient data exist to extend this analysis to higher latitudes;

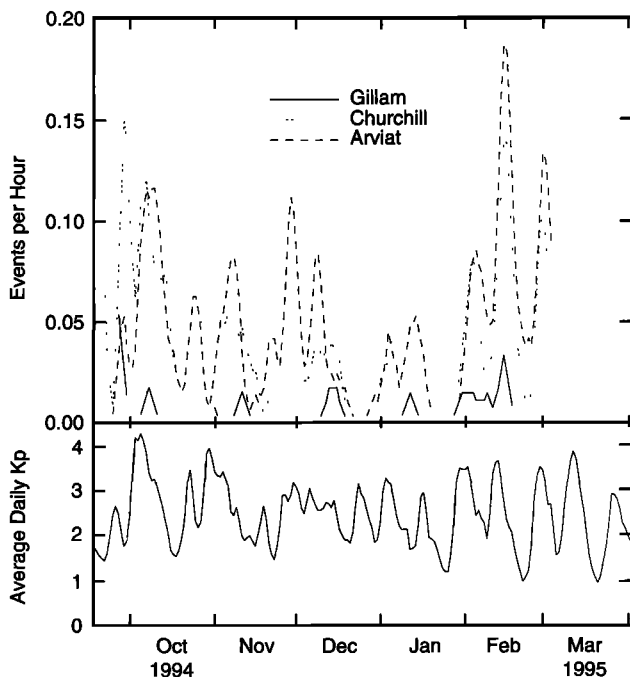


Figure 2. Occurrence rates of MF burst emissions at three stations between September 1994 and April 1995. For comparison, a light solid trace shows a 7-day running average of the daily sum Kp indices during the same interval. During this solar minimum time period, MF burst emissions occur more frequently at 69° – 71° invariant latitude than at lower latitude. As expected for a substorm phenomenon, MF bursts are correlated with Kp .

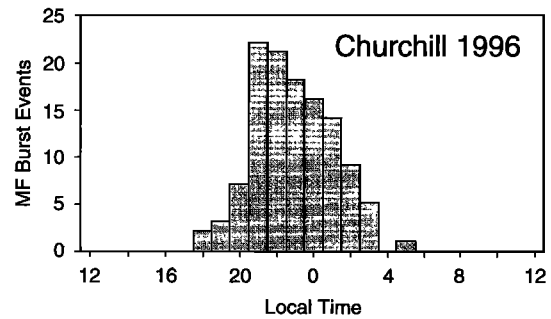


Figure 3. MF burst events detected at Churchill during 1996, as a function of time of day. (Midnight magnetic local time is 0635 UT.)

however, case studies suggest that the occurrence rate is lower at Baker Lake and Taloyoak, so that 69° – 71° probably represents the peak in the latitude distribution of these emissions. The occurrence of MF burst emissions varies episodically, with peaks in the occurrence rates at all stations characteristically separated by intervals of 27 days. For reference, Figure 2 displays the Kp index for the same 6-month period. Peaks in MF burst occurrence rates correspond to relatively high Kp , consistent with previous observations of the close correlation between MF bursts, substorm onsets, and auroral hiss. Furthermore, based on this 6-month interval, the MF burst occurrence rates tend to be higher near the equinoxes than at winter solstice.

Figure 3 shows the total number of MF bursts recorded at Churchill in 1996 as a function of time of day. MF bursts are most common in the premidnight hours. The diurnal occurrence pattern is strikingly similar to that reported for impulsive auroral hiss (for example, Figure 1 of Morgan [1977]), an observation which suggests a close association between these two phenomena. MF bursts are absent under daylight conditions during this period.

The initial study of MF bursts included evidence that these bursts vary in amplitude on short time scales. On occasion, spectrograms of MF burst events recorded with the NPR appear speckled, implying that the bursts flicker on and off on timescales comparable to the ~ 10 ms sample period of the NPR [Weatherwax *et al.*, 1994]. Clearly the NPR, while useful for detecting MF burst events, does not resolve them. In April 1996, we conducted a 3-week campaign in Churchill, Manitoba, in which the downconverting receiver was operated interactively to capture waveforms associated with auroral radio emissions. The primary goal of these observations was to better document auroral roar fine structure [Shepherd *et al.*, 1997]. Because of their shorter timescale, MF burst emissions were hard to identify in the real-time plots quickly enough to tune the downconverting receiver to capture them, but despite this difficulty one MF burst event was captured with the downconverting receiver. The time resolution of the

downconverting receiver (0.1 ms) is 2 orders of magnitude faster than the sample rate of the previous measurements.

Figure 4a shows a spectrogram of MF bursts recorded with the NPR during 0414:30–0423:30 UT on April 15, 1996. Figure 4b shows a spectrogram recorded with the downconverting receiver for 19.5 seconds, starting at 0417:19 UT, and Figure 4c shows the amplitude of the downconverted signal, averaged with a 1.2-ms window. During this interval the center frequency of the downconverter is 1998 kHz, implying that the vertical axis of the downconverted spectrogram corresponds to 1993–2003 kHz. Numerous modulations in the MF burst intensity occur during the selected 19.5-s interval, but there is no evidence of frequency structure within the 10-kHz bandwidth of the downconverting receiver.

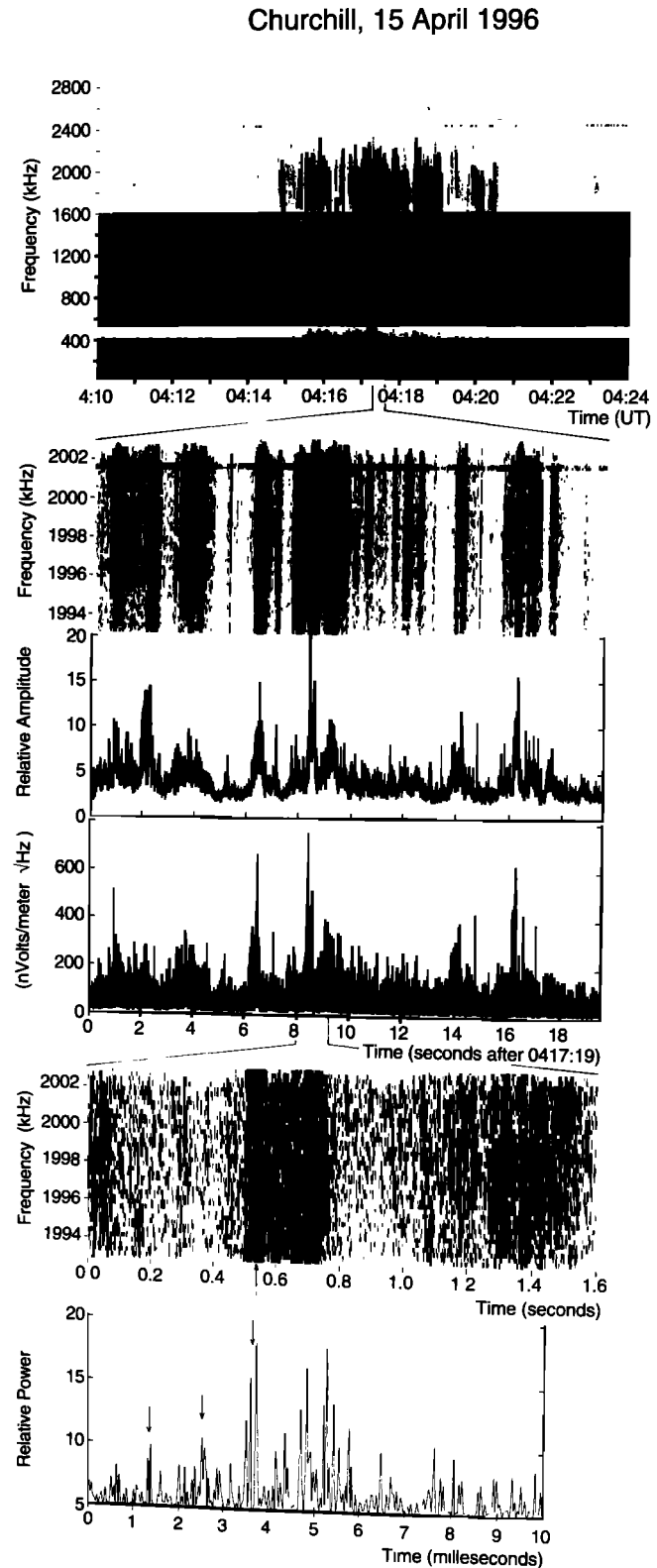
Figure 4d shows the output of the 2000-kHz channel from the FPR which has the same bandwidth (10 kHz) and time resolution (1.2 ms) as the time-averaged downconverted signal amplitude displayed in Figure 4c. The two waveforms resemble each other except for the peaks in the downconverted signal amplitude at 2–3 s in the record which are an artificially injected time code signal and should be ignored. Unlike the downconverter, the FPR output is calibrated and therefore provides absolute signal amplitudes associated with the bursts. At the 1.2-ms resolution of the FPR, the MF burst spectral density in this 10-kHz band ranges from 0.1 to 0.6 $\mu\text{V}/\text{m}\sqrt{\text{Hz}}$. However, at millisecond resolution, the MF burst is not fully resolved; the peaks in the waveforms shift by 10–20 dB between individual samples.

The 10-kHz bandwidth of the downconverting receiver provides even higher time resolution. Figure 4e shows an expanded spectrogram derived from 1.6 s (0417:26.0–0417:27.6) of downconverter waveform data, corresponding to the interval indicated by vertical lines below Figure 4d. Each Fourier transform making up the spectrogram in Figure 4e corresponds to 4 ms of data. An interval of enhanced power spectral density covering the full 10-kHz frequency range of the receiver occurs 0.5 s into the record and lasts approximately 250 ms. No frequency fine structure is observable.

The bottom panel, Figure 4f, shows the highest time resolution available: the square of the waveform from

the downconverting receiver is plotted versus time with no time averaging for the 10 ms interval indicated by an arrow below Figure 4e. At this resolution, MF burst is observed to be composed of short duration wave packets. For example, one wave packet indicated by an arrow at 3.5–3.8 ms in the record consists of three peaks in the rectified waveform lasting 0.3 ms (1-1/2 cycles

Figure 4. (a) A 0–2.9 MHz spectrogram showing MF bursts observed on April 15, 1996; (b) a spectrogram of a 10-kHz band centered at 1998 KHz, for a 19-s interval beginning at 0417:19 UT; (c) 1.2 ms averages of the amplitude of the 10-kHz band centered at 1998 kHz; (d) the amplitude of the FPR channel centered at 2000 kHz and sampled at 1.2-ms intervals; (e) an expanded spectrogram of the 10-kHz band centered at 1998 kHz, for a selected 1.6-s interval; and (f) the square of the waveform of the 10-kHz bandwidth signal centered on 1998 kHz, plotted with full time resolution for a selected 10-ms interval. Arrows in the bottom panel indicate MF burst wave packets of duration 100–300 μs . These are quasiperiodic with spacing ~ 1.5 ms.



at the downconverted frequency, or about 600 cycles at the ~ 2 -MHz center frequency of the downconverted band). Other wave packets, also indicated by arrows in Figure 4f, have similar durations. The wave packets appear quasiperiodic, with a period of ~ 1.25 ms in this example. Extrapolating from the 10-ms interval in Figure 4f, the vertical streaks which appear as individual bursts in the low-resolution spectrograms of MF bursts (Figures 1 and 4a), as well as the enhanced power spectral density feature shown in Figure 4e which lasts a few hundred milliseconds, actually contain of hundreds of short duration wave packets. The timescales of these wave packets, fractions of a millisecond, are almost 2 orders of magnitude shorter than the upper bound inferred from lower resolution measurements.

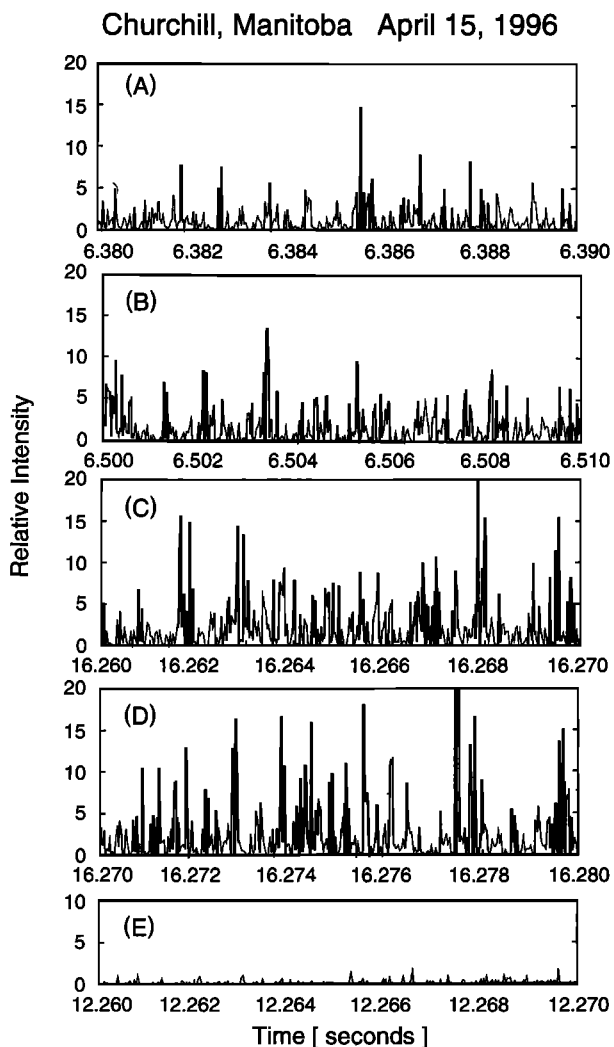


Figure 5. The relative intensity of the 10-kHz band centered at 1998 MHz, for five selected 10-ms intervals within the April 15, 1996, MF burst event shown in Figure 4. In the top two examples, the wave packets are separated by 1–1.5 ms; in the next two panels, the wave packets have larger amplitude, are more tightly packed, and sometimes overlap. The bottom panel shows the background level at a time when no MF burst occurs.

Figure 5 shows full-resolution waveforms measured with the downconverting receiver, in the same format as Figure 4f. The relative intensity scale on the y-axes is identical for all five panels and for Figure 4f. Figures 5a and 5b show 10-ms intervals starting at 6.38 and 6.50 s in Figures 4b–4d during which the MF burst wave packets are distinct from one another and quasi-periodic, with periods in the range 1–1.5 ms. In contrast, Figures 5c and 5d show examples in which the wave packets are closer together, even overlapping. When the wave packets are more frequent, their amplitudes tend to be larger, averaging 10–15 units in Figures 5c and 5d but only 5–10 units in Figures 5a and 5b. For comparison, Figure 5e shows a waveform from a time interval when no MF bursts occur, showing that during the MF bursts, the wave packets greatly exceed the background level, and some fluctuations in intensity above the background are observed in the intervals between the short-duration wave packets.

Figure 6 shows FPR data from a 600-ms interval during an MF burst event at 0741:16 UT on April 14, 1996. For two selected frequencies within the MF burst, 2.3 and 2.6 MHz, wave power spectral density (PSD) versus time is displayed with no averaging, 1.2 ms per sample. The two frequencies are sampled sequentially, 0.3 ms apart. During this time, MF bursts are observed over a frequency range extending from below 2.3 MHz to above 2.6 MHz. Sometimes peaks in the PSD occur simultaneously at both frequencies, as for example at 7.9 s in the record. At other times a peak in PSD is registered only at one of the two frequencies. For example, near 8.06 s in the record, a peak at 2.3 MHz corresponds to a valley between two peaks at 2.6 MHz. This signature could occur if the wave packets comprising MF burst are broadband but last about 0.3 ms, the interval separating the samples of the two frequencies; in that case, the wave packet may be present during the 2.3-MHz sample but absent during the 2.6-MHz sample. The duration of the wave packets inferred from this under-sampling hypothesis is consistent with that measured independently with the downconverting receiver.

Figure 7 illustrates a correlation between auroral MF burst and auroral hiss recorded 0527–0541 UT on February 18, 1995, at Arviat (71.4° invariant). The decrease in the amplitude of AM broadcast band signals (535–1605 kHz) between the beginning and end of the record indicates the onset of D region absorption, a signature of the substorm expansion phase with which MF burst and impulsive auroral hiss are associated. The MF bursts occur between 1400 and 2950 kHz, and the auroral hiss extends from the lowest frequency measured (30 kHz) to above 900 kHz. The time resolution of these NPR measurements does not fully resolve the impulsive radio emissions, but the correlation between groups of impulses is obvious in Figure 7, as it is in the example of Figure 1a. The MF bursts illustrated in Figures 1 and 7 are exceptionally intense, but the correlation between auroral hiss and MF burst seen in

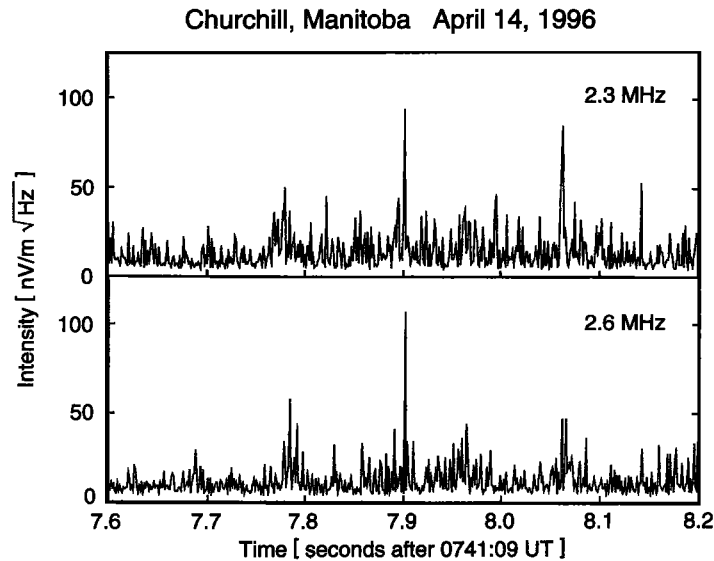


Figure 6. The amplitude at two frequencies as a function of time during an MF burst event observed at Churchill on April 14, 1996, using the FPR with 1.2-ms resolution. The appearance of amplitude peaks in one frequency but not the other is consistent with wave packet timescales the order of 0.3 ms, the interval between the samples of the two frequencies.

Figures 1 and 7 is typical of weaker MF burst events as well. Although auroral hiss often occurs without MF burst, auroral hiss is nearly always present when MF burst occurs. In the few examples out of hundreds in

which MF burst is not accompanied by LF auroral hiss, it cannot be excluded that VLF auroral hiss occurs at frequencies below the lower bound of the receiver.

To explore the correlation between auroral hiss and MF burst at shorter timescales, Figure 8a shows an MF burst recorded on April 14, 1996, and Figures 8b and 8c show 24-ms running averages of two FPR channels, 430 kHz and 2.0 MHz, for a 19.5 s interval starting at 0757:29 UT. The correlation between these time series does not appear strong: 2.0-MHz time series corresponding to MF burst shows more peaks in power spectral density than the 430-kHz time series which corresponds to the auroral hiss; nevertheless, peaks in the 430-kHz auroral hiss intensity line up with peaks in the 2.0-MHz MF burst intensity, though not always the other way around. The poor correlation probably results because auroral hiss amplitude usually decreases with increasing frequency in the LF range, so that at 430 kHz, the hiss mostly lies below the noise level of the instrument. The high time resolution data in Figure 8 are consistent with a correlation between auroral hiss and MF burst on short timescales but do not establish such a correlation. Simultaneous high time resolution VLF hiss and MF burst data are required in order to establish whether these two phenomena are correlated on the timescale of the MF burst wave packets.

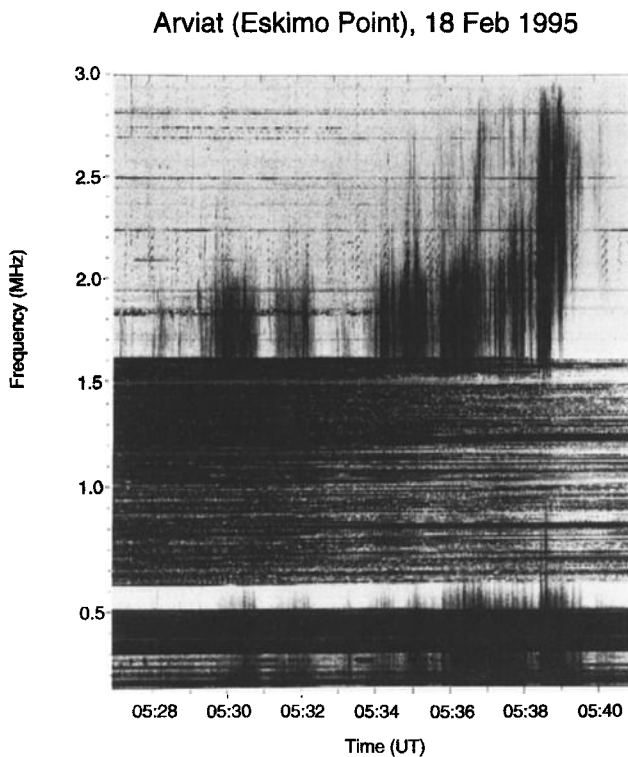


Figure 7. A 0.15–3.00 MHz spectrogram recorded at Arviat during 0527–0541 UT on February 18, 1995. The MF burst in the frequency range 1.5–2.9 MHz is correlated with the auroral hiss in the frequency range 30 kHz to 0.9 MHz.

4. Discussion

Since the first observation of auroral MF burst in October 1993, hundreds more events have been detected at many observatories. The frequency of the MF bursts ranges from about 1.3 to 4.5 MHz. For reference, the ionospheric electron gyrofrequency above Churchill,

Churchill, Manitoba, April 14, 1996

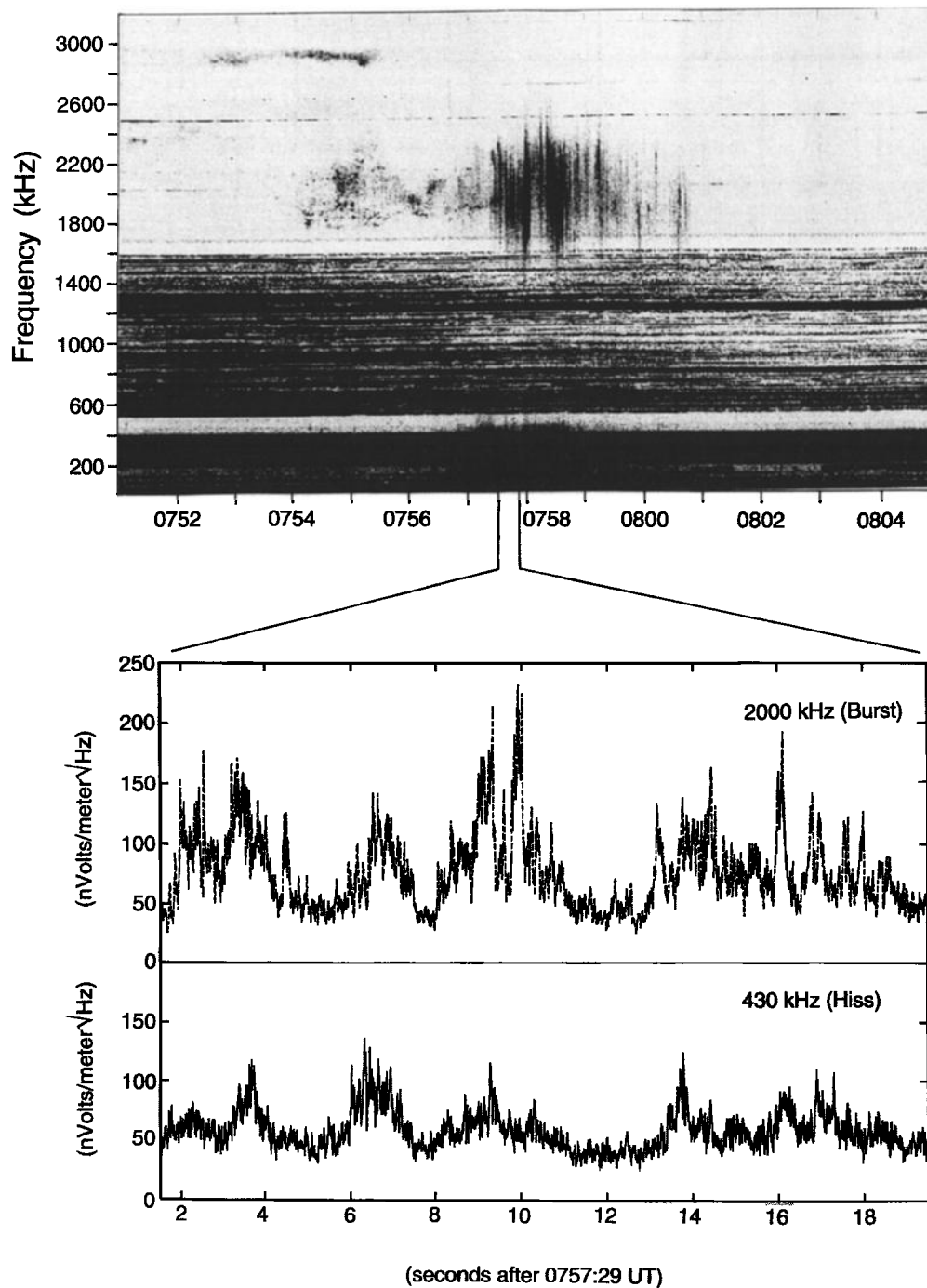


Figure 8. (a) A 0–3.2 MHz spectrogram showing an MF burst event recorded at Churchill, Manitoba, on 14 April, 1996; (b) the amplitude of a 10-kHz band centered at 2.0 MHz, corresponding to the middle of the MF burst and averaged with a 24-ms window; (c) the amplitude in a 10-kHz band centered at 430 kHz, corresponding to the auroral hiss.

Manitoba, ranges from 1.61 MHz at 100 km to 1.07 MHz at 1000 km. Recent data leave no doubt that the spectrum of MF burst has a null near 2.9 MHz (possibly corresponding to twice the ionospheric electron gyrofrequency near 300 km altitude) suggested by previous statistical studies [Weatherwax *et al.*, 1994]. Surprisingly,

on short timescales MF burst is organized into wave packets of duration 100–300 μs . At timescales of seconds to minutes, MF burst is correlated with impulsive auroral hiss, with both emissions occurring during the expansion phase of auroral substorms. The correlation between auroral hiss and MF burst at the time scales

of the MF burst wave packets has not been established. MF burst is sometimes localized, with intensity differing by more than 35 dB between observations 200 km apart. Auroral hiss and roar are often similarly localized.

The power spectral density of MF burst emissions at 2.0–2.6 MHz, averaged over 1 ms, ranges from 100 to 750 nV/m $\sqrt{\text{Hz}}$. This number represents an average over multiple 100–300 μs wave packets, the most intense of which have power spectral densities in the range 1–2 $\mu\text{V}/\text{m}\sqrt{\text{Hz}}$. Assuming a bandwidth of 0.5–1.0 MHz, the field strength at ground level associated with the most intense wave packets is about 1 mV/m. If the source lies at 500 km altitude, this field strength implies peak powers of 1000 W for an isotropic source, or much less for a beamed source. For example, a 15° beam would imply ~ 30 W. The energy in an individual 300 μs wave packets would be as large as 0.3 J (10 mJ) for the isotropic case (15° beam case). The average power is lower than the peak power by a factor of 2–10. For comparison, the average power of a 10 \times 300 km auroral arc is typically $\sim 10^7$ W. However, if the MF burst source is confined to a tiny section of the arc, then the generation mechanism must be fairly efficient; for example, if the source were confined to a 10 \times 10 km section of the arc and the emission were isotropic, the required efficiency is the order of one percent.

Although closely associated with auroral hiss, MF bursts occur at frequencies above the electron cyclotron frequency and hence cannot propagate in the whistler mode as does auroral hiss. Figure 9 illustrates a possible mechanism for generation of MF bursts. The vertical axis represents altitude, and the horizontal axis represents frequency. The dark trace represents a typical profile of either the electron plasma frequency or the

upper hybrid frequency in the auroral ionosphere. At higher altitudes than shown here, precipitating auroral electrons generate auroral hiss, probably via mechanisms described in the literature [e.g., Maggs, 1976]. If the distribution of the auroral electrons at ionospheric altitudes is characterized by a bump-on-tail, Langmuir waves would be excited at the local plasma frequency as indicated by crosses in the figure. Alternatively, a loss cone feature in the electron distribution function would destabilize upper hybrid waves. In either case these electrostatic waves must convert to electromagnetic waves in order to propagate to the ground.

In this model, the upper frequency bound of the MF burst corresponds to the maximum plasma frequency or maximum upper hybrid frequency in the ionosphere, either in the E peak or in the F peak as shown in Figure 9. The lower frequency bound might correspond to the plasma or upper hybrid frequency at the altitude where the electron distribution is no longer unstable due to collisional damping or due to degradation of the nonthermal feature in the distribution. Alternatively, if radiation originates at the bottomside of the F layer and if there is significant precipitation-induced ionization in the D or E regions, the blanketing effect of these layers may determine the lower frequency limit of the MF burst as shown in Figure 9. The observed upper frequency bounds of MF burst, ranging from 2 to 4.5 MHz, are similar to the range of peak plasma or upper hybrid frequencies in the auroral ionosphere, and the observed lower bound exceeds the electron gyrofrequency at F region altitudes and is comparable to a typical maximum plasma frequency in an enhanced E region.

Simultaneous ground-based radiowave and incoherent scatter radar observations at Sondrestrom, Greenland, provide evidence that sufficiently high plasma densities occur in the ionosphere during MF burst events. Figure 10 shows swept receiver data from March 23, 1996, when the maximum frequency of the MF burst increases from 2 MHz to 3 MHz between 0107 and 0108 UT. The bottom panels present plots of the electron density measured during consecutive radar antenna scans in the magnetic meridian. These plots show electron density contours versus altitude and north-south distance from the radar facility. The first scan (labeled A) covers approximately 0103–0107 UT, and the second scan (labeled B) covers approximately 0107–0111 UT. The maximum electron density measured by the radar jumps from a little over $5 \times 10^4 \text{ cm}^{-3}$ ($f_{pe} \approx 2$ MHz) during the first scan to about $3.5 \times 10^5 \text{ cm}^{-3}$ ($f_{pe} \approx 5$ MHz) during the second scan, with the enhanced density observed in a narrow region south of Sondrestrom and associated with an auroral arc as confirmed by all-sky camera images (M. McCready, personal communication, 1997). These data show that at all times the maximum plasma frequency somewhere in the ionosphere within a few hundred kilometers of the radar facility exceeds the maximum frequency of the simultaneously observed MF burst.

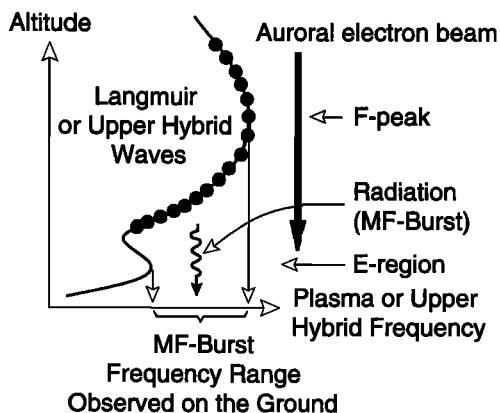


Figure 9. A sketch of a possible mechanism for generating MF burst emissions: in the bottomside of the F region, auroral electrons generate Langmuir or upper hybrid waves over a range of altitudes corresponding to the range of frequencies in MF burst. These electrostatic waves must then convert to electromagnetic waves in order to propagate to the ground.

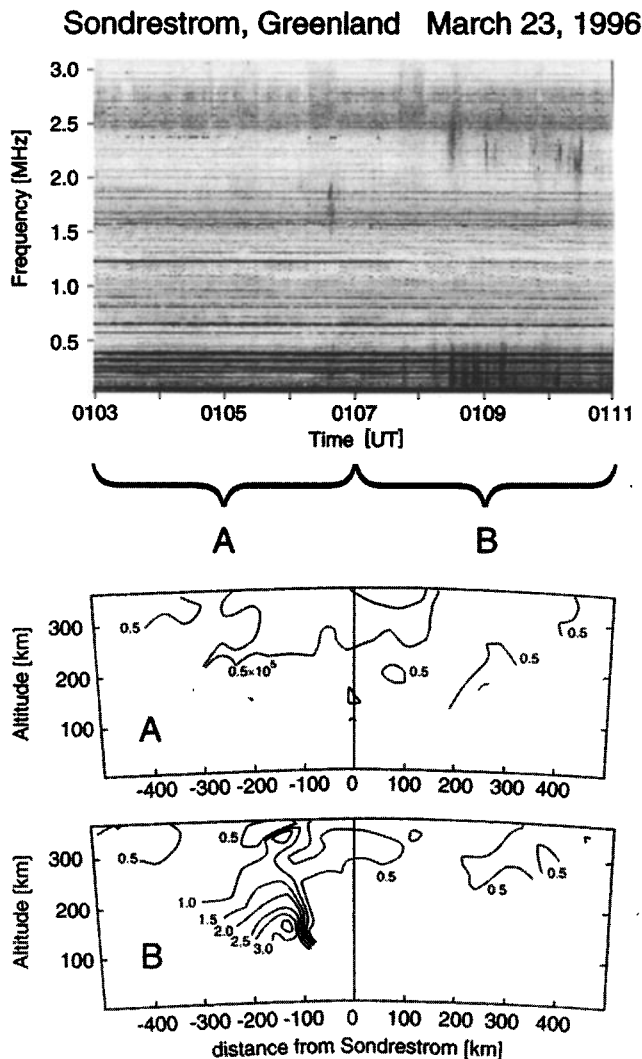


Figure 10. Swept receiver and incoherent scatter radar data recorded at Sondrestrom, Greenland, on March 23, 1996. The top panel shows auroral hiss and MF burst emissions extending up to 3 MHz. The bottom panels show electron density contours, as a function of altitude and north-south distance from the radar facility, measured during consecutive radar antenna scans in the magnetic meridian: the first scan (labeled A) covers approximately 0103–0107 UT, and the second scan (labeled B) covers approximately 0107–0111 UT. These data confirm that at all times the maximum plasma frequency somewhere in the ionosphere within a few hundred kilometers of the radar facility exceeds the maximum frequency of the simultaneously observed MF burst.

The generation mechanism depicted in Figure 9 is similar to one proposed for auroral roar, except that auroral roar may be associated with upper hybrid waves generated at a particular altitude rather than Langmuir or upper hybrid waves generated over a range of altitudes. For both auroral roar and MF burst, the outstanding theoretical difficulty is to explain the mode conversion required by these models. Four possibilities are nonlinear wave-wave coupling or parametric decay,

as occurs stimulated electromagnetic emissions [e.g., Thidé *et al.*, 1983]; linear mode conversion on a steep density gradient, as postulated for generation of terrestrial continuum radiation at the plasmopause [e.g., Oya, 1971; Jones, 1976]; mode conversion of upper hybrid waves in a region of density irregularities, analogous to a similar process at the lower hybrid frequency described by Bell and Ngo [1990]; or propagation through the Z mode radio window, which also requires a density gradient [e.g., Budden, 1985]. While there is a direct topological connection between the Langmuir wave and the L-mode, this connection occurs where the phase velocity is far too high for the waves to be resonant with any electron beam.

Another outstanding difficulty in MF burst theory is to explain the null in the spectrum near twice the ionospheric electron gyrofrequency. This feature might be attributed to cyclotron absorption by ambient electrons along the propagation path, but the mystery is why electrons from a relatively narrow range of altitudes, 277–315 km in the case of Figure 1a, contribute to the absorption. Auroral roar occurs in the same relatively narrow frequency range and perhaps affects the electron distribution and enhances cyclotron absorption there.

The wave packet nature of the MF bursts might be a consequence of either nonlinear wave processes or bursty structure in the causative auroral electrons. There are no observations of electron distribution functions with 100- μ s time resolution. However, Ergun *et al.* [1996] recently reported FAST satellite observations of auroral hiss at several thousand kilometers altitude showing that hiss sometimes consists of individual wave packets called whistler solitary structures, of duration 100–300 μ s. Furthermore, these whistler solitary structures are sometimes periodic on timescales of the local ion gyroperiod. Electrons accelerated by the whistler solitary structures at several thousand kilometers would be too dispersed to generate the 100–300 μ s structure in MF bursts at F region altitudes unless the acceleration were constrained to an unrealistically narrow energy range. Therefore, if the whistler solitons are responsible for accelerating electrons which generate MF burst by the mechanism shown in Figure 9, the acceleration must occur at low altitudes. If one associates the occasional 1–1.5 ms periodicity in the MF burst wave packets with ion cyclotron frequency in the region of the whistler solitary waves which accelerate the electrons, then these must be at ionospheric altitudes. Future high time resolution ground based or in situ measurements resolving 100–300 μ s structure in MF burst and auroral hiss simultaneously will provide a means to probe the relationship between them.

Sotnikov *et al.* [1996] propose an alternative generation mechanism for MF burst which exploits the energy in the perpendicular velocity component of the auroral electrons rather than the parallel component. In their model, electron acoustic waves mediate the energy

transfer between the electrons and the electromagnetic waves. Generation of such electron acoustic waves has been observed in electron beams generated artificially in the ionosphere during active experiments [Sotnikov *et al.*, 1995]. This mechanism also relies on some means for converting the electrostatic wave energy into electromagnetic waves.

In conclusion, the most dramatic result of recent experiments is the resolution of the short time structure of the MF bursts which are composed of wave packets lasting only 100-300 μ s. Models for the generation mechanism must account for this fine structure. Other features which need to be accounted for are the frequency range (1.3-4.5 MHz), the null in the spectrum near 2.9 MHz, the observation of wave intensities differing by more than 35 dB at stations 200 km apart, and the correlation between MF burst and auroral hiss. The last observation suggests a close connection between MF burst and auroral hiss.

Acknowledgments. The authors thank the operators at the CANOPUS observatories for their reliable support of the Dartmouth radio receivers. In particular, we thank the staff at Churchill Northern Studies Center for their support and hospitality when Dartmouth personnel visited for several weeks to make detailed observations, and we thank Fokke Creutzberg, Don Wallis, and Terry Hughes for providing and interpreting plots of CANOPUS magnetometer and riometer data. We thank Mary McCready and SRI for processing and interpreting incoherent scatter radar data in support of our operations at Sondrestrom. Three Dartmouth undergraduates played key roles in the design and construction of the downconverting receiver: Rajive Jayawardhane, David Rinehart, and Jeremy Eisen. Dartmouth undergraduates Barnaby Olson and Samantha Abeyratne contributed to the statistical data analysis presented in the paper. This research is supported by NSF grant ATM-9316126 to Dartmouth College.

The editor thanks H. G. James and P. J. Kellogg for their assistance in evaluating this paper.

References

Bell, T.F., and H.D. Ngo, Electrostatic lower hybrid waves excited by electromagnetic whistler mode waves scattering from planar field-aligned plasma density irregularities, *J. Geophys. Res.*, **95**, 149, 1990.
 Budden, K.G., *The Propagation of Radio Waves*, Cambridge Univ. Press, New York, 1985.

Ergun, R.E., et al., Initial results from the FAST mission: DC turbulence, VLF waves, and AKR, *Trans. AGU*, **77** (46), Fall Meet. Suppl., F625, 1996.
 Helliwell, R. A., *Whistlers and Related Ionospheric Phenomena*, Stanford Univ. Press, Stanford, Calif., 1965.
 Jones, D., Source of terrestrial non-thermal radiation, *Nature*, **260**, 686, 1976.
 Kellogg, P. J., and S. J. Monson, Radio emissions from the aurora, *Geophys. Res. Lett.*, **6**, 297, 1979.
 LaBelle, J., A.T. Weatherwax, M.L. Trimpi, R. Brittain, R.D. Hunsucker, and J.V. Olson, The spectrum of radio noise at ground level during substorms, *Geophys. Res. Lett.*, **21**, 2749, 1994.
 LaBelle, J., M.L. Trimpi, R. Brittain, and A.T. Weatherwax, Fine structure of auroral roar emissions, *J. Geophys. Res.*, **100**, 21953, 1995.
 Maggs, J.E., Coherent generation of VLF hiss, *J. Geophys. Res.*, **81**, 1707, 1976.
 Morgan, M.G., Auroral hiss on the ground at $L \approx 4$, *J. Geophys. Res.*, **82**, 2387, 1977.
 Oya, H., Conversion of electrostatic plasma waves into electromagnetic waves: numerical calculation of the dispersion relation for all wavelengths, *Radio Sci.*, **6**, 1131, 1971.
 Sazhin, S.S., K. Bullough, and M. Hayakawa, Auroral hiss: A review, *Planet. Space Sci.*, **41**, 153, 1993.
 Shepherd, S.G., J. LaBelle, M. Trimpi, and R. Brittain, Further investigation of auroral roar fine structure, *Trans. AGU*, **77** (17), Spring Meet. Suppl., S190, 1996.
 Sotnikov, V., D. Schriver, M. Ashour-Abdalla, J. Ernst-meyer, and N. Myers, Excitation of electron acoustic waves by a gyrating electron beam, *J. Geophys. Res.*, **100**, 19765, 1995.
 Sotnikov, V., D. Schriver, M. Ashour-Abdalla, and J. LaBelle, Generation of auroral radio waves by a gyrating electron beam, *Trans. AGU*, **77** (46), Fall Meet. Suppl., F544, 1996.
 Thidé, B., H. Derblom, A. Hedberg, H. Kopka, and P. Stubbe, Observations of stimulated electromagnetic emissions in ionospheric heating experiments, *Radio Sci.*, **18**, 851, 1983.
 Weatherwax, A. T., Ground-based observations of auroral radio emissions, Ph.D. thesis, Dartmouth College, Hanover, N.H., 1994.
 Weatherwax, A. T., J. LaBelle, and M. L. Trimpi, A new type of auroral radio emission observed at medium frequencies (1350-3700 kHz) using ground-based receivers, *Geophys. Res. Lett.*, **21**, 2753, 1994.

J. LaBelle, S. G. Shepherd, and M. L. Trimpi, Department of Physics and Astronomy, 6127 Wilder Laboratory, Dartmouth College, Hanover, NH 03755.

(Received March 24, 1997; revised June 27, 1997; accepted June 30, 1997.)